IJISET - International Journal of Innovative Science, Engineering & Technology, Vol. 2 Issue 11, November 2015.
www.ijiset.com
ISSN 2348 – 7968

Numerical Simulation for Steady Incompressible Laminar Fluid Flow and Heat Transfer inside T-Shaped Cavity Using Stream Function And Vorticity

Hassan Nasr Ahamed Ismail[1], Aly Maher Abourabia[2], Abd El Rahman Ali Saad[3], A .El Desouky A .[4]

[1]Department of Basic Engineering Sciences, Benha Faculty of Engineering, Benha University

[2]Department of Mathematics, Faculty of Science, Menoufiya University

[3]Department of Mathematics and Physics, Shoubra Faculty of Engineering, Benha University

[4]Department of Basic Engineering Science, Benha Faculty of Engineering, Benha University

Abstract

For numerical simulations, we will use finite difference approximation to solve non-dimensional Navier-Stokes equations (NSEs) which has forms stream functions and vorticity. The fluid flow inside T - shaped cavity is movement subject to laminar flow. The equations of motion and energy of the viscous fluid flow apply for a steady state of incompressible fluids. The fluid mechanics under this boundary is simulated in two dimensional domains" x and y". Under these boundary conditions we simulate the streamlines, vorticity, temperature distribution and velocity vector in x-y plane. The head part of the cavity is driven by the horizontal velocity in x-direction. During the motion of the fluid inside the cavity, some vertices vorticity will appear, these vertices indicate that position and change its positions under changing the Reynolds numbers. The viscous fluid motion is simulated under the Prandtl number is equal 1.96 and the Reynolds numbers 1, 50, 100, 150 and increasing the Reynolds number by interval 50 and the maximum Reynolds number is 2000.

Keywords: *Navier-Stokes Equations, laminar flow, T - shaped cavity, incompressible viscous fluid, finite difference method.*

1. Introduction

The cavity flow simulation was introduced in early 1982 used finite difference method (FDM) [1]. Conventional FDM with new perspective is applied to the simulation of lid driven flow in a 2-D, rectangular, deep cavity. Results are presented in streamlines pattern for deep cavity flow at steady state for various Reynolds numbers. The predicted result from FDM with new perspective gives more improvement results as grid mesh increases [2]. The 2-D lid driven square cavity flow is simulated using finite difference method with non-uniform meshing for various Reynolds numbers. Special non-uniform finite difference approximation is developed. Where 50×50 non-uniform meshing was used to simulate the streamline patterns, center of the vortex, horizontal and vertical midsection velocity [3]. It is found that a plethora of vortex patterns can be generated with different aspect ratios and directions of motion of the walls. More recently, Perumal and Dass [4-5] investigated the flow driven by parallel and antiparallel motion of two facing walls in a two-sided lid-driven square cavity at different Reynolds numbers, using finite difference method and Lattice Boltzmann method. In [6] investigated the characteristics of incompressible viscous flow inside a two sided lid driven deep cavity with its two opposite walls moving with a uniform velocity in parallel and in anti-parallel direction at different Reynolds numbers by finite difference method. The parallel and antiparallel motion results are studied for the streamline and vorticity contours with the variation of Reynolds number [6]. The flow inside the two sided lid driven cavity is simulated using third order upwind compact finite difference scheme based on flux difference splitting in combination with artificial compressibility approach. Unlike single lid driven cavity, there is free shear layer and two symmetric secondary eddies growing in size directly with Reynolds numbers for parallel wall motion. However, for anti-parallel wall motion the eddy structure changes [7]. The mixed convection heat transfer and fluid flow behaviors in a lid-driven square cavity filled with a high Prandtl number at low Reynolds number is studied using thermal Lattice Boltzmann method (TLBM). The results are presented as velocity and temperature profiles as well as stream function and temperature contours are present in the study [8]. The algorithm used to compute the flow in a two-sided 2D lid-driven cavity where, besides wall shear, free shear flow is also encountered. The present work is concerned with the computation of two-sided lid-driven square cavity flows by Finite Difference Method [9]. Another classic example is the case where a flow is induced by the tangential movement of two facing cavity boundaries with uniform velocities. If the two facing walls move in the same direction, it is termed the parallel wall

E-mail: (1) am_abourabia@yahoo.com
(2) eng_eldesoky@yahoo.com

ISSN 2348 – 7968

motion and if in the opposite direction, it is termed anti-parallel wall motion. Kuhlmann and other investigators [10-11-12] have done several experiments and computational works on two-sided lid-driven rectangular cavity with various aspect ratios. [13] The effect of inclination angle on the heat transfer rate and flow pattern inside a lid-driven square cavity with different mixed convection parameter has been studied. The driven cavity contains an incompressible fluid bounded by a square enclosure and the flow is driven by a uniform translation of the top lid and it serves as a means through which any numerical scheme can be validated [14].

h	Distance between two successive nodes
i	Unit vector in horizontal direction
j	Unit vector in vertical direction
K	Coefficient of thermal conductivity
p	Non-Dimensional pressure
T	Temperature
u	Non-Dimensional horizontal velocity
v	Non-Dimensional vertical velocity
x	Non-Dimensional horizontal direction
y	Non-Dimensional vertical direction
C_v	Specific heat at constant volume per unit mass
N_x	Node number in x-direction
P_r	Prandtl number
Re	Reynolds number
T_c	Cold temperature
T_h	Hot temperature
U_0	Characteristic velocity
α	Characteristic length in x-direction
β	Characteristic length in y-direction
γ	Aspect ratio between α and β
θ	Non-Dimensional temperature
μ	Coefficient of dynamic viscosity
ρ	Density
ψ	Non-Dimensional stream function
ω	Non-Dimensional vorticity

Table 1: Table of symbols

2. Problem Statement

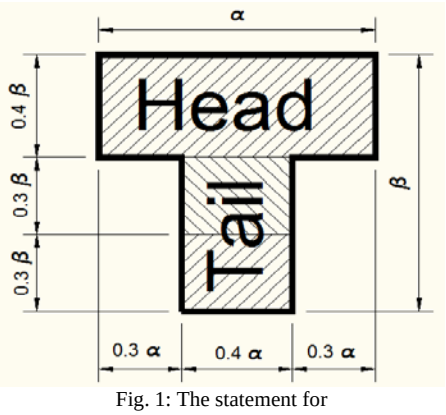

Fig. 1: The statement for T-shaped cavity.

The Navier-Stokes equations solve under the boundary conditions which has a T - shaped cavity. The cavity indicated in Fig.1 has two parts. The top part called the head and the lower part called the tail. The physical structure of the cavity itself is in dimensionless parameters and solving under aspect ratio equal to 1" α =1 and β = 1".

Now, simulate the structure of T-shaped cavity as present in Fig. 2

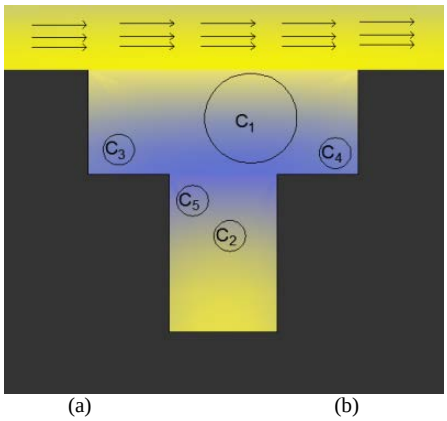

(a) (b)

Fig. 2: The structure of T-shaped cavity

Fig. 2 present the structure of T-shaped cavity. Where the upper part of the head is driven by characteristic horizontal uniform constant velocity in x-direction. The large circle area is the location of primary vertex C_1 And drive all the secondary vertices C_3 and C_4. During the Reynolds numbers are increasing the tertiary vertex C_5 is appear.

3. Governing Equations

For laminar incompressible steady state flow, the governing equations for NSEs " continuity equation, Momentum Equation in x and y direction and energy Equation"[15-16] can be written with the symbol (*) as

$$\frac{\partial u^*}{\partial x^*} + \frac{\partial v^*}{\partial y^*} = 0 \quad (1)$$

$$\rho^*\left(u^*\frac{\partial u^*}{\partial x^*} + v^*\frac{\partial u^*}{\partial y^*}\right) = -\frac{\partial p^*}{\partial x^*} + \mu^*\left(\frac{\partial^2 u^*}{\partial x^{*2}} + \frac{\partial^2 u^*}{\partial y^{*2}}\right) \quad (2)$$

$$\rho^*\left(u^*\frac{\partial v^*}{\partial x^*} + v^*\frac{\partial v^*}{\partial y^*}\right) = -\frac{\partial p^*}{\partial y^*} + \mu^*\left(\frac{\partial^2 v^*}{\partial x^{*2}} + \frac{\partial^2 v^*}{\partial y^{*2}}\right) \quad (3)$$

$$\rho^* {C_v}^*\left(u^*\frac{\partial T^*}{\partial x^*} + v^*\frac{\partial T^*}{\partial y^*}\right) = K^*\left(\frac{\partial^2 T^*}{\partial x^{*2}} + \frac{\partial^2 T^*}{\partial y^{*2}}\right) \quad (4)$$

ISSN 2348 – 7968

Using non-dimensional parameter which used to convert Navier-Stokes equations to non-dimensional forms can written as,

$$x = \frac{x^*}{\alpha}, y = \frac{y^*}{\beta}, \gamma = \frac{\alpha}{\beta}, u = \frac{u^*}{U_0}, v = \frac{v^*}{U_0}, p = \frac{P^*}{\rho\, {U_0}^2},$$
$$\theta = \frac{T - T_c}{T_h - T_c}, \psi = \frac{\psi^*}{U_0\, \alpha}, \omega = \frac{\omega^*\, \alpha}{U_0} \quad (5)$$

$$\left(\frac{\partial u}{\partial x} + \gamma \frac{\partial v}{\partial y}\right) = 0 \quad (6)$$

$$\left(u\frac{\partial u}{\partial x} + \gamma v \frac{\partial u}{\partial y}\right) = \frac{-\partial p}{\partial x} + \frac{1}{Re}\left[\left(\frac{\partial^2 u}{\partial x^2}\right) + \gamma^2\left(\frac{\partial^2 u}{\partial y^2}\right)\right] \quad (7)$$

$$\left(u\frac{\partial v}{\partial x} + \gamma v \frac{\partial v}{\partial y}\right) = -\gamma\frac{\partial p}{\partial y} + \frac{1}{Re}\left[\left(\frac{\partial^2 v}{\partial x^2}\right) + \gamma^2\left(\frac{\partial^2 v}{\partial y^2}\right)\right] \quad (8)$$

$$\left(u\frac{\partial \theta}{\partial x} + \gamma v \frac{\partial \theta}{\partial y}\right) = \frac{1}{P_r Re}\left(\frac{\partial^2 \theta}{\partial x^2} + \gamma^2\frac{\partial^2 \theta}{\partial y^2}\right) \quad (9)$$

Where, Reynolds number and Prandtl number and equals

$$Re = \frac{\rho^*\, U_0\, \alpha}{\mu^*}, \qquad P_r = \frac{{C_v}^*\, \mu^*}{K^*} \quad (10)$$

Stream function and vorticity equations during the horizontal and vertical velocities has formed [17]

$$u^* = \frac{\partial \psi^*}{\partial y^*}, \qquad v^* = -\frac{\partial \psi^*}{\partial x^*}, \qquad \omega^* = \frac{\partial v^*}{\partial x^*} - \frac{\partial u^*}{\partial y^*} \quad (11)$$

From Eq. (11) and non-dimensional parameter (5), non-dimensional stream function and vorticity has form.

$$u = \gamma\frac{\partial \psi}{\partial y}, \qquad v = -\frac{\partial \psi}{\partial x}, \qquad \omega = -\left(\frac{\partial^2 \psi}{\partial x^2} + \gamma^2\frac{\partial^2 \psi}{\partial y^2}\right) \quad (12)$$

From the Eq. (7) and Eq. (12) and multiply $-(\partial/\partial y)$ in x-momentum, the new equation has form

$$-u\frac{\partial}{\partial y}\frac{\partial u}{\partial x} - v\frac{\partial}{\partial y}\frac{\partial u}{\partial y} = \frac{\partial}{\partial y}\frac{\partial p}{\partial x} - \frac{1}{Re}\frac{\partial}{\partial y}\left[\frac{\partial^2 u}{\partial x^2} + \frac{\partial^2 u}{\partial y^2}\right] \quad (13)$$

From the Eq. (8) and Eq. (12) and multiply $-(\partial/\partial x)$ in y-momentum, the new equation has form

$$u\frac{\partial}{\partial x}\frac{\partial v}{\partial x} + v\frac{\partial}{\partial x}\frac{\partial v}{\partial y} = -\frac{\partial}{\partial x}\frac{\partial p}{\partial y} + \frac{1}{Re}\frac{\partial}{\partial x}\left[\frac{\partial^2 v}{\partial x^2} + \frac{\partial^2 v}{\partial y^2}\right] \quad (14)$$

By adding Eq. (13) in Eq. (14) and from the stream function and vorticity Eq. (12), the momentum equation has form

$$\left(\frac{\partial \psi}{\partial y}\frac{\partial \omega}{\partial x} - \frac{\partial \psi}{\partial x}\frac{\partial \omega}{\partial y}\right) = \frac{1}{Re}\left[\frac{\partial^2 \omega}{\partial x^2} + \frac{\partial^2 \omega}{\partial y^2}\right] \quad (15)$$

From the Eq. (9) and from the stream function and Eq. (12), the energy equation has form.

$$\left(\frac{\partial \psi}{\partial y}\frac{\partial \theta}{\partial x} - \frac{\partial \psi}{\partial x}\frac{\partial \theta}{\partial y}\right) = \frac{1}{P_r\, Re}\left(\frac{\partial^2 \theta}{\partial x^2} + \frac{\partial^2 \theta}{\partial y^2}\right) \quad (16)$$

4. The Boundary Condition

The boundary conditions for dimensionless stream function, horizontal velocity, vertical velocity and temperature indicated in Fig. 3 are as follows.

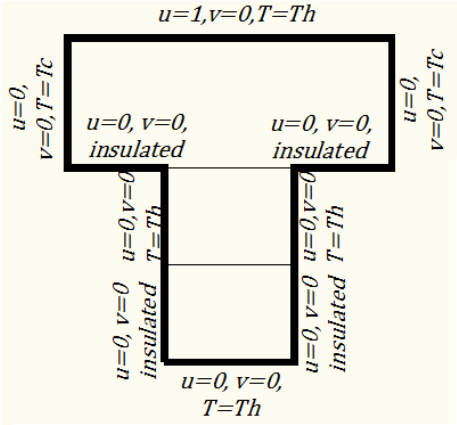

Fig. 3: T-shaped boundary conditions.

$$\psi = 0, u = 0, v = 0 \text{ and } \theta = 1 \text{ at } x = 0.3\alpha \text{ and } 0.3\beta \le y \le 0.6\beta, \; x = 0.7\alpha \text{ and } 0.3\beta \le y \le 0.6\beta \quad (17)$$

$$\psi = 0, u = 0, v = 0 \text{ and } \frac{\partial \theta}{\partial x} = 0 \text{ at } x = 0.7\alpha \text{ and } 0 \le y \le 0.3, \; x = 0.3\alpha \text{ and } 0 \le y \le 0.3\beta \quad (18)$$

$$\psi = 0, u = 0, v = 0 \text{ and } \theta = 0 \text{ at } x = \alpha \text{ and } 0.6\,\beta \le y \le \beta, \; x = 0 \text{ and } 0.6\,\beta \le y \le \beta \quad (19)$$

$$\psi = 0, u = 0, v = 0 \text{ and } \frac{\partial \theta}{\partial y} = 0 \text{ at } y = 0.6\,\beta \text{ and } 0.7\alpha \le x \le \alpha, \; y = 0.6\,\beta \text{ and } 0 \le x \le 0.3\alpha \quad (20)$$

$$\psi = 0, u = 1, v = 0, \text{and } \theta = 1 \text{ at } y = \beta \text{ and } 0 \le x \le \alpha \quad (21)$$

$$\psi = 0, u = 0, v = 0, \text{and } \theta = 1 \text{ at } y = 0 \text{ and } 0.3\alpha \le x \le 0.7\alpha \quad (22)$$

ISSN 2348 – 7968

5. Two Dimensional Grid Generation for the Two Cases

The grid generation is important for any kind of simulation. For finite difference method, the walls and interior areas of the T - shaped cavity in Fig. 4 are divided to equal grids which have the same offset between the grid and each other.

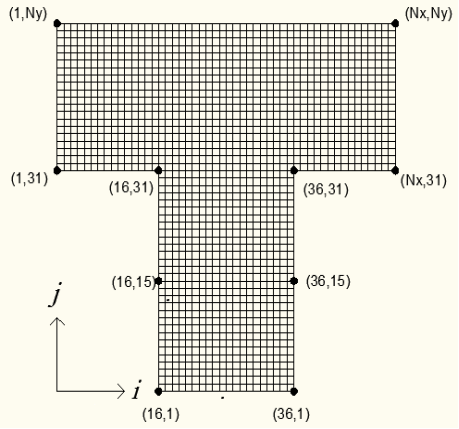

Fig. 4: The grid generation for cavity.

In i and j directions, the grids are innumerate from 1 to N_x and from 1 to N_y respectively.

Where,

$$i \in N \ and \ j \in N$$

This cavity solved under the number of grids $N_x = 51$ and $N_y = 51$ in i-direction and j-direction respectively. The distance between any grids "h" is equal to 0.02 in the horizontal or vertical direction during the equation

$$\boldsymbol{h = \frac{\alpha}{N_x - 1} = \frac{\beta}{N_y - 1}} \tag{23}$$

6. Finite Difference Approximation

We use the finite difference approximate to solve steady state incompressible Navier-Stokes equations for T-shaped boundaries and for the interior area of these cavities to approximate the stream function, vorticity, temperature and the two velocities in horizontal and vertical axis [18].

$$\omega_{i,j} = \frac{-1}{h^2}\left[\psi_{i+1,j} + \psi_{i-1,j} + \psi_{i,j+1} + \psi_{i,j-1} - 4\psi_{i,j}\right] \tag{24}$$

$$\frac{1}{4\,h^2}\left[(\psi_{i,j+1} - \psi_{i,j-1})(\omega_{i+1,j} - \omega_{i-1,j})\right] - \frac{1}{4\,h^2}\left[(\psi_{i+1,j} - \psi_{i-1,j})(\omega_{i,j+1} - \omega_{i,j-1})\right] = \frac{1}{Re\,h^2}\left[\omega_{i+1,j} + \omega_{i-1,j} + \omega_{i,j+1} + \omega_{i,j-1} - 4\omega_{i,j}\right] \tag{25}$$

$$u_{i,j} = \frac{1}{2h}(\psi_{i,j+1} - \psi_{i,j-1}) \tag{26}$$

$$v_{i,j} = \frac{1}{2h}(\psi_{i+1,j} - \psi_{i-1,j}) \tag{27}$$

$$\frac{1}{4}\left[(\psi_{i,j+1} - \psi_{i,j-1})(\theta_{i+1,j} - \theta_{i-1,j})\right] - \frac{1}{4}\left[(\psi_{i+1,j} - \psi_{i-1,j})(\theta_{i,j+1} - \theta_{i,j-1})\right] = \frac{1}{Re\,P_r}\left[\theta_{i+1,j} + \theta_{i-1,j} + \theta_{i,j+1} + \theta_{i,j-1} - 4\theta_{i,j}\right] \tag{28}$$

The Prandtl number can be assume equal to 1.96 to approximate the temperature equation for the two cases. The system of equations applied to the head part at i and j is present in the interval

$$2 \le i \le N_x - 1 \quad and \quad 32 \le j \le N_y - 1$$

While for the tail part i and j is present in the interval

$$17 \le i \le 35 \quad and \quad 2 \le j \le 31$$

7. Results and Discussions

A. Plotting the Fluid Properties

Using symbolic Mathematical software for plotting the velocity vector profiles, streamline profiles, vorticity profiles, temperature distribution profiles, inside T-shaped cavity at various Reynolds numbers

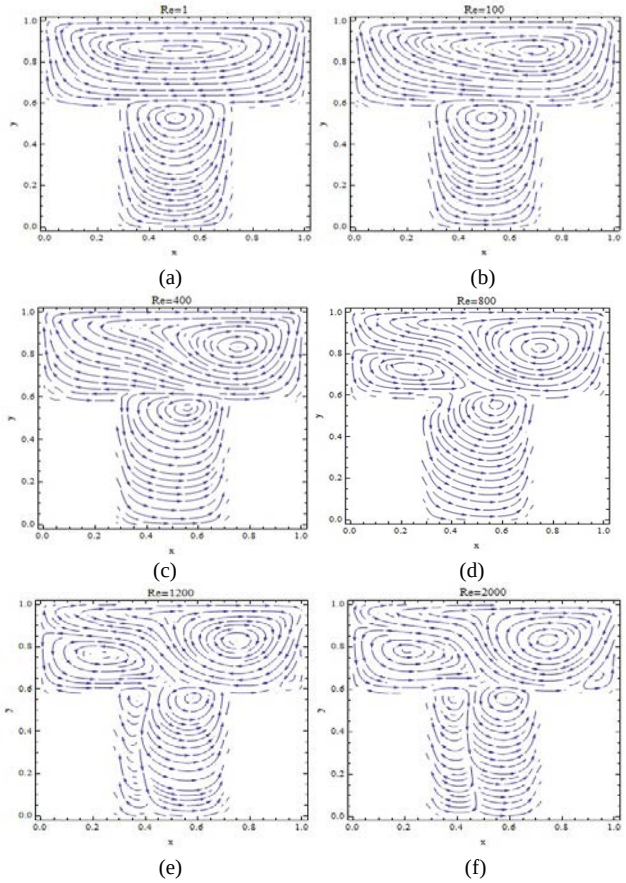

Fig. 5: Non-Dimensional velocity vector at (a) Re=1, (b) Re=100, (c) Re=400, (d) Re=450, (e) Re=500, (f) Re=800, (g) Re=1200, (h) Re=2000.

ISSN 2348 – 7968

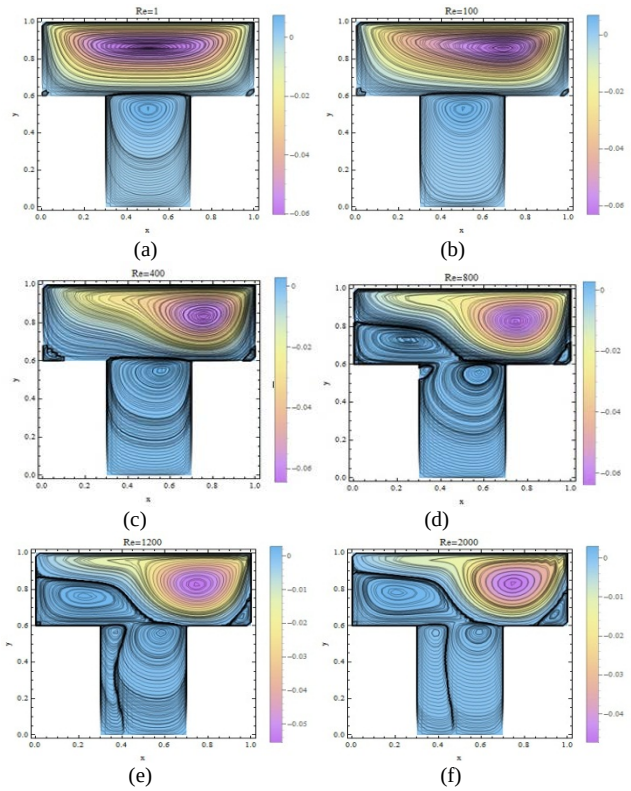

Fig. 6: Non-Dimensional streamlines at (a) Re=1, (b) Re=100, (c) Re=400, (d) Re=800, (e) Re=1200, (f) Re=2000.

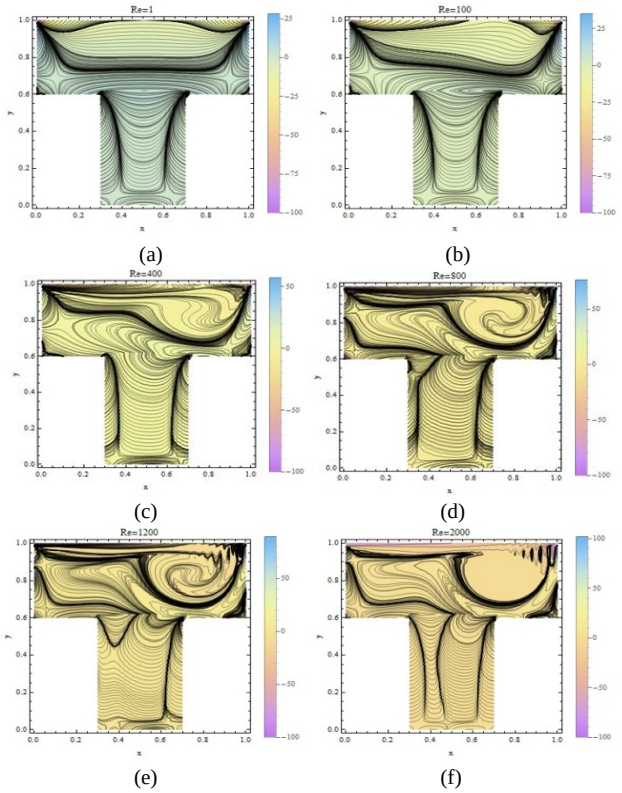

Fig. 7: Non-Dimensional vorticity profile at (a) Re=1, (b) Re=100, (c) Re=400, (d) Re=800, (e) Re=1200, (f) Re=2000.

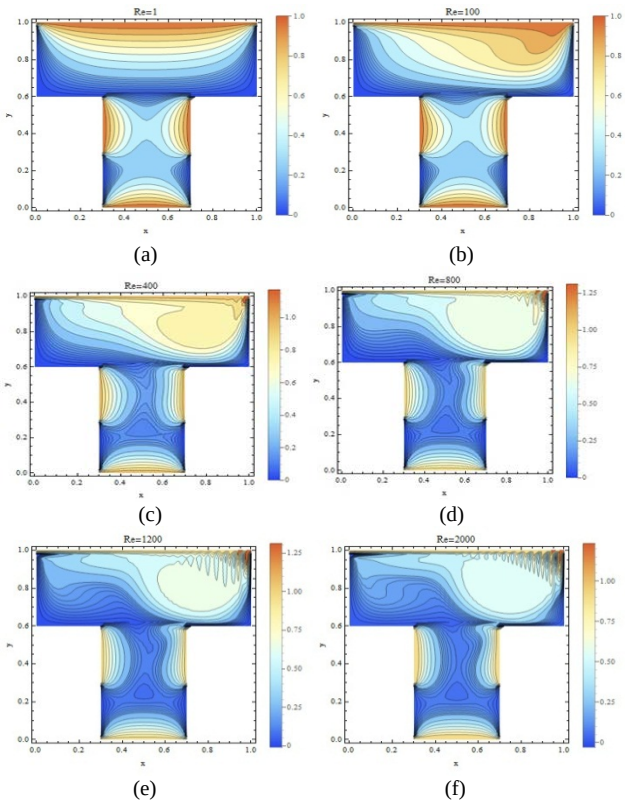

Fig. 8: Non-Dimensional temperature distribution profile at (a) Re=1, (b) Re=100, (c) Re=400, (d) Re=800, (e) Re=1200, (f) Re=2000.

B. The Velocities about the Centerlines Technique for the Three Cases

In this technique, it is observed that the positions of the primary and some vorticity vortexes by two steps. The first step occurred by fitting curve between the horizontal centerline of the cavity with the *v*-velocities approximations in the horizontal centerline of the cavity. From this curve, can observation x-coordinates points at which the *v*-velocities are equal to zero. The second step occurred by fitting curve between the vertical centerline of the cavity with the *u*-velocities approximations in the vertical centerline of the cavity. From this curve, can observation y-coordinates points at which the *u*-velocities are equal to zero.

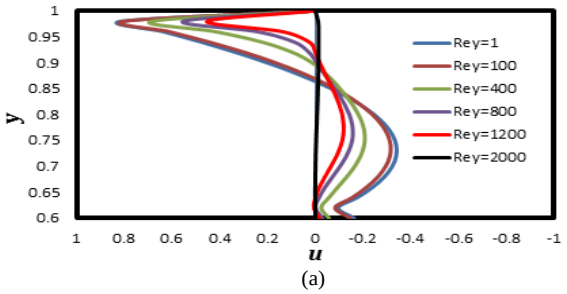

(a)

ISSN 2348 – 7968

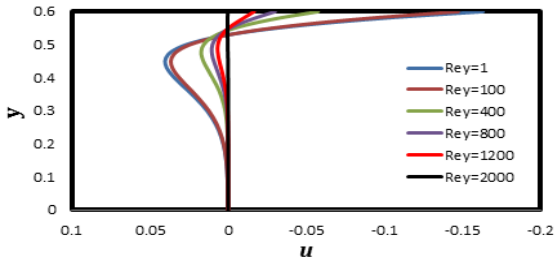

(b)

Fig. 13**:** *u*-velocity along vertical centerline of (a) head part and (b) tail part.

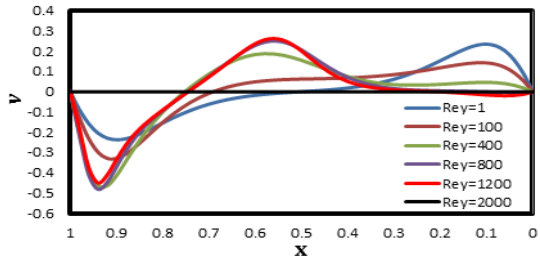

(a)

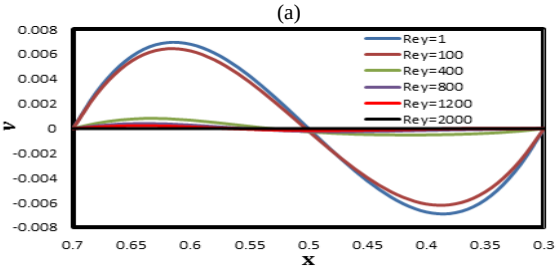

(b)

Fig. 14**:** *v* -velocity along vertical centerline of (a) head part and (b) tail part

C. The Maximum and Minimum Stream Function Technique for Three Cases

In this technique we used the results of the stream function approximation to observe the points of vorticity vortexes. The position of minimum value of stream function is the primary vertex and the tertiary vertex, but the positions of the secondary vertex at the maximum value of stream function.

Primary vertex "C_1"					
Re	***x***	***y***	ψ_{min}	ω	θ
1	0.5	0.86	-0.060328	-4.663970	0.586347
50	0.64	0.86	-0.061365	-4.977770	0.678908
100	0.7	0.86	-0.063144	-5.433670	0.747130
150	0.72	0.86	-0.064349	-5.616780	0.753628
200	0.74	0.86	-0.064686	-5.778100	0.752148
250	0.76	0.84	-0.065117	-5.905730	0.750189
300	0.76	0.84	-0.065383	-5.816500	0.739782
350	0.76	0.84	-0.065318	-5.686660	0.730354
400	0.76	0.84	-0.065014	-5.534500	0.720911
450	0.76	0.84	-0.064551	-5.387330	0.711552
500	0.76	0.84	-0.0634385	-5.16182	0.546344
550	0.76	0.84	-0.063439	-5.161820	0.693930
600	0.74	0.82	-0.062916	-5.278180	0.685239
650	0.74	0.82	-0.062423	-5.201730	0.677338
700	0.74	0.82	-0.061904	-5.128900	0.669811
750	0.74	0.82	-0.061356	-5.058450	0.662560
800	0.74	0.82	-0.060781	-4.990990	0.655588
850	0.74	0.82	-0.060179	-4.925960	0.648856
900	0.74	0.82	-0.059550	-4.863030	0.642335
950	0.74	0.82	-0.058896	-4.801990	0.635996
1000	0.74	0.82	-0.058224	-4.742630	0.629804
1050	0.74	0.82	-0.057539	-4.684930	0.623738
1100	0.74	0.82	-0.056848	-4.628920	0.617787
1150	0.74	0.82	-0.056159	-4.574640	0.611953
1200	0.74	0.82	-0.055476	-4.522020	0.606234
1250	0.74	0.82	-0.054802	-4.471060	0.600639
1300	0.74	0.82	-0.054138	-4.421970	0.595191
1350	0.74	0.82	-0.053487	-4.374220	0.589858
1400	0.74	0.82	-0.052849	-4.327940	0.584654
1450	0.74	0.82	-0.052225	-4.282950	0.579569
1500	0.74	0.82	-0.051615	-4.239320	0.574613
1550	0.74	0.82	-0.051920	-4.261135	0.577091
1600	0.74	0.82	-0.050437	-4.155940	0.565075
1650	0.74	0.82	-0.051179	-4.208538	0.571083
1700	0.74	0.82	-0.049314	-4.077510	0.556021
1750	0.74	0.82	-0.050246	-4.143024	0.563552
1800	0.74	0.82	-0.048246	-4.003700	0.547422
1850	0.74	0.84	-0.049246	-4.073362	0.555487
1900	0.74	0.84	-0.047336	-4.091290	0.549839
1950	0.74	0.84	-0.048291	-4.082326	0.552663
2000	0.74	0.84	-0.047813	-4.086808	0.551251

(a)

ISSN 2348 – 7968

Secondary vertex " C_3"					
Re	***x***	***y***	ψ_{min}	ω	θ
1	0.02	0.62	8.7*10^-6	0.113106	0.003385
50	0.02	0.62	7.5*10^-6	0.071441	0.002524
100	0.02	0.62	5.9*10^-6	0.041797	0.003772
150	0.02	0.62	4.4*10^-6	0.029050	0.004096
200	0.02	0.62	3.6*10^-6	0.024437	0.004194
250	0.02	0.62	3.1*10^-6	0.018158	0.004192
300	0.02	0.62	2.6*10^-6	0.011511	0.004125
350	0.02	0.64	2.2*10^-6	0.005189	0.004032
400	0.04	0.64	6.9*10^-6	0.032194	0.015748
450	0.04	0.64	0.000029	0.204215	0.065413
500	0.28	0.66	0.000174	0.275085	0.089522
550	0.26	0.68	0.000373	0.345006	0.109715
600	0.26	0.7	0.000603	0.472083	0.129541
650	0.26	0.7	0.000868	0.436384	0.122404
700	0.24	0.72	0.001116	0.536508	0.141673
750	0.26	0.72	0.001370	0.553064	0.134112
800	0.24	0.74	0.001581	0.662116	0.152839
850	0.24	0.74	0.001820	0.642143	0.148886
900	0.24	0.74	0.002018	0.621691	0.146134
950	0.24	0.74	0.002182	0.601035	0.144339
1000	0.24	0.76	0.002329	0.746382	0.154554
1050	0.24	0.76	0.002480	0.723745	0.152363
1100	0.22	0.76	0.002604	0.688404	0.157617
1150	0.22	0.76	0.002706	0.671404	0.156546
1200	0.22	0.76	0.002789	0.654729	0.155720
1250	0.22	0.76	0.002856	0.638559	0.155062
1300	0.22	0.76	0.002908	0.622953	0.154517
1350	0.22	0.78	0.002961	0.746148	0.156709
1400	0.22	0.78	0.003013	0.728623	0.155567
1450	0.22	0.78	0.003054	0.711737	0.154543
1500	0.22	0.78	0.003087	0.695485	0.153609
1550	0.22	0.78	0.003109	0.680198	0.152760
1600	0.22	0.78	0.003131	0.664910	0.151910
1650	0.2	0.78	0.003145	0.659943	0.153746
1700	0.2	0.78	0.003158	0.654975	0.155581
1750	0.2	0.78	0.003164	0.644084	0.154609
1800	0.2	0.78	0.003169	0.633193	0.153637
1850	0.2	0.78	0.003102	0.624934	0.153497
1900	0.2	0.78	0.003035	0.616676	0.153357
1950	0.2	0.78	0.002968	0.608417	0.153216
2000	0.2	0.78	0.002901	0.600158	0.153076

(b)

Secondary vertex " C_4"					
Re	***x***	***y***	ψ_{min}	ω	θ
1	0.98	0.62	8.7*10^-6	0.114707	0.003527
50	0.98	0.62	9.8*10^-6	0.155079	0.008183
100	0.98	0.62	0.000012	0.188232	0.012150
150	0.98	0.62	0.000015	0.209013	0.015226
200	0.98	0.62	0.000018	0.214617	0.017598
250	0.98	0.62	0.000022	0.212098	0.019538
300	0.98	0.62	0.000027	0.204063	0.021151
350	0.98	0.62	0.000031	0.191841	0.022489
400	0.98	0.64	0.000043	0.511068	0.046153
450	0.98	0.64	0.000055	0.496431	0.047744
500	0.98	0.64	0.000067	0.478297	0.049011
550	0.98	0.64	0.000080	0.455376	0.049959
600	0.98	0.64	0.000091	0.430283	0.050678
650	0.98	0.64	0.000103	0.403320	0.051195
700	0.96	0.64	0.000124	1.193790	0.106190
750	0.96	0.64	0.000156	1.188270	0.106754
800	0.96	0.64	0.000187	1.177910	0.107013
850	0.96	0.64	0.000216	1.162970	0.107001
900	0.96	0.64	0.000245	1.143700	0.106746
950	0.96	0.64	0.000272	1.120430	0.106279
1000	0.96	0.64	0.000298	1.093610	0.105631
1050	0.96	0.64	0.000323	1.063710	0.104834
1100	0.96	0.66	0.000355	1.828160	0.136157
1150	0.96	0.66	0.000395	1.781700	0.133785
1200	0.96	0.66	0.000433	1.732100	0.131337
1250	0.96	0.66	0.000468	1.680040	0.128851
1300	0.96	0.66	0.000501	1.625990	0.126355
1350	0.96	0.66	0.000532	1.570790	0.123892
1400	0.96	0.66	0.000561	1.514840	0.121490
1450	0.96	0.66	0.000588	1.458660	0.119176
1500	0.96	0.66	0.000613	1.402580	0.116970
1550	0.94	0.66	0.000649	1.990875	0.144846
1600	0.94	0.66	0.000686	2.579170	0.172721
1650	0.94	0.66	0.000737	2.515165	0.169254
1700	0.94	0.66	0.000787	2.451160	0.165786
1750	0.94	0.66	0.000831	2.386085	0.162665
1800	0.94	0.66	0.000874	2.321010	0.159543
1850	0.94	0.66	0.000902	2.256248	0.157286
1900	0.94	0.66	0.000930	2.191485	0.155029
1950	0.94	0.66	0.000958	2.126723	0.152771
2000	0.94	0.66	0.000985	2.061960	0.150514

(c)

ISSN 2348 – 7968

Secondary vertex " C_2"					
Re	***x***	***y***	ψ_{min}	ω	θ
1	0.5	0.54	0.007519	2.278080	0.214805
50	0.5	0.54	0.007411	2.231680	0.227436
100	0.54	0.54	0.006841	2.069490	0.234069
150	0.52	0.54	0.005896	1.830480	0.238737
200	0.52	0.54	0.004981	1.603470	0.221870
250	0.54	0.54	0.004327	1.470250	0.225298
300	0.54	0.54	0.003792	1.366240	0.200458
350	0.56	0.54	0.003246	1.292170	0.198242
400	0.56	0.56	0.003067	1.622890	0.194827
450	0.56	0.56	0.002937	1.574810	0.190878
500	0.56	0.56	0.002838	1.538590	0.187748
550	0.58	0.56	0.002747	1.548010	0.228057
600	0.58	0.56	0.002680	1.519690	0.224795
650	0.58	0.56	0.002616	1.492310	0.221484
700	0.58	0.56	0.002553	1.464280	0.218118
750	0.58	0.56	0.002490	1.435420	0.214964
800	0.58	0.56	0.002425	1.405110	0.211784
850	0.58	0.56	0.002356	1.373900	0.208135
900	0.58	0.56	0.002289	1.340990	0.205215
950	0.58	0.56	0.002223	1.307330	0.202571
1000	0.58	0.56	0.002156	1.274430	0.199548
1050	0.58	0.56	0.002091	1.242540	0.196633
1100	0.58	0.56	0.002029	1.212380	0.193617
1150	0.58	0.56	0.001971	1.183770	0.190960
1200	0.58	0.56	0.001918	1.156890	0.188662
1250	0.58	0.56	0.001869	1.131850	0.186490
1300	0.58	0.56	0.001823	1.107940	0.184648
1350	0.58	0.56	0.001782	1.085730	0.183147
1400	0.58	0.56	0.001744	1.065000	0.181745
1450	0.58	0.56	0.001709	1.045790	0.180440
1500	0.58	0.56	0.001677	1.027580	0.179437
1550	0.58	0.56	0.001648	1.010967	0.178540
1600	0.58	0.56	0.001618	0.994353	0.177643
1650	0.58	0.56	0.001592	0.979499	0.176861
1700	0.58	0.56	0.001566	0.964645	0.176079
1750	0.58	0.56	0.001543	0.951288	0.175388
1800	0.58	0.56	0.001520	0.937930	0.174697
1850	0.58	0.56	0.001140	0.703448	0.131023
1900	0.58	0.56	0.000760	0.468965	0.087349
1950	0.58	0.56	0.001019	0.650783	0.123364
2000	0.58	0.56	0.001279	0.832601	0.159379

(d)

Tertiary vertex '' C_5''					
Re	***x***	***y***	ψ_{min}	ω	θ
700	0.32	0.58	-0.000001	-0.077710	0.576943
750	0.32	0.58	-0.000007	-0.071828	0.579022
800	0.34	0.58	-0.000019	-0.124870	0.396444
850	0.34	0.58	-0.000030	-0.128889	0.399106
900	0.36	0.58	-0.000042	-0.163522	0.288874
950	0.36	0.58	-0.000056	-0.169464	0.291156
1000	0.36	0.58	-0.000067	-0.173333	0.293327
1050	0.36	0.58	-0.000076	-0.175543	0.295327
1100	0.36	0.56	-0.000085	-0.102576	0.393228
1150	0.36	0.56	-0.000092	-0.102908	0.394085
1200	0.38	0.56	-0.000099	-0.123874	0.287691
1250	0.38	0.56	-0.000106	-0.124644	0.288027
1300	0.38	0.56	-0.000111	-0.124815	0.288338
1350	0.38	0.56	-0.000115	-0.124523	0.288628
1400	0.38	0.56	-0.000118	-0.123900	0.288827
1450	0.38	0.56	-0.000120	-0.123025	0.288939
1500	0.38	0.56	-0.000121	-0.121933	0.289080
1550	0.38	0.56	-0.000121	-0.120646	0.289128
1600	0.38	0.56	-0.000122	-0.119359	0.289176
1650	0.38	0.56	-0.000122	-0.117921	0.289121
1700	0.38	0.56	-0.000121	-0.116482	0.289065
1750	0.38	0.56	-0.000121	-0.114980	0.288923
1800	0.38	0.56	-0.000120	-0.113478	0.288781
1850	0.38	0.56	-0.000121	-0.112161	0.287073
1900	0.38	0.56	-0.000122	-0.110845	0.285365
1950	0.38	0.56	-0.000124	-0.109528	0.283657
2000	0.38	0.56	-0.000125	-0.108211	0.281949

(e)

Table 2: Simulation of vertices under the various of Reynolds numbers for (a) vertex " C_1", (b) vertex " C_3", (c) vertex " C_4", (d) vertex " C_2"and (e) vertex " C_5".

Table (2) presents Simulation of vertices for case I under the various of Reynolds numbers and Show its locations and the value of the stream function and vorticity. For vertex C_1 and C_5, has a negative sign of the stream function and vorticity for any Reynolds number, this means that the vortices rotating clockwise. For the vertices " C_3", " C_4" and " C_2", has a positive sign of the stream function and vorticity for any Reynolds number, this means that the vortices rotating counterclockwise.

ISSN 2348 – 7968

8. Conclusions

The viscous fluid flow and energy inside T-shaped cavity was simulated for different Reynolds numbers and Prandtl number is equal 1.96. Using the finite difference method to solve Navier-Stokes equations which for the stream functions and vorticity to simulate the fluid mechanics. The equations of motion of the viscous fluid flow subject to laminar flow are applied in steady state for incompressible fluid with the boundary conditions. We simulate the streamline, vorticity, temperature distribution and velocity vector in x-y plane. The head part of the cavity is driven by the horizontal velocity in x-direction. During these motions, some vertices vorticity has appeared and observed that position and change its positions under changed the Reynolds number.

References

[1] K.N. Ghia and C.T. Shin, "High-Resolutions for incompressible flow using the Navier–Stokes equations and a multigrid method", Journal of Computational Physics, Vol. 48, PP. 367-411, (1982)

[2] M.S. Idris and N.M.N.M. Ammar, "2-D Deep Cavity Flow, Lid Driven Using Conventional Method With New Perspective", National Conference in Mechanical Engineering Research and Postgraduate Studies, Faculty of Mechanical Engineering, UMP Pekan, Kuantan, Pahang, pp. 550-558, (2010).

[3] M.S.Idris and C.S.N. Azwadi,"Numerical Investigation of 2-D Lid Driven Cavity Flow Emphasizing Finite Difference Method of Non Uniform Meshing", National Conference in Mechanical Engineering Research and Postgraduate Students, FKM Conference Hall, UMP, Kuantan, Pahang, Malaysia, pp. 91-98, (2010).

[4] Perumal, Anoop K.Dass,"Simulation of incompressible flows in two-sided lid-driven square cavities. Part I – FDM", CFD Letters, Issue 1, Vol. 2(1), pp. 13-24, (2010).

[5] Perumal, Anoop K.Dass,"Simulation of incompressible flows in two-sided lid-driven square cavities, Part II – LBM", CFD Letters, Issue 1, Vol. 2(1), pp. 25-38, (2010).

[6] Perumal, "Simulation of Flow in Two-Slid Lid Driven Deep Cavities by Finite Difference Method", Journal of applied science in the thermodynamics and fluid mechanics, Vol. 6(1), (2012)

[7] A. Munir, M. Rizwan, M. Khan and A.Shah, "Simulation of Incompressible Flow in Two Sided Lid Driven Cavity using Upwind Compact Scheme", CFD Letters, Vol. 5(3), pp. 57-66, (2013).

[8] M. A. Taher, S. C. Saha, Y. W. Lee, H. D. Kim, "Numerical Study of Lid-Driven Square Cavity with Heat Generation Using LBM", American Journal of Fluid Dynamics, Vol. 3(2), PP. 40-47, (2013).

[9] N. Kumar, J.C. Kalita and A.K. Dass, "Computation of Two-Sided Lid-Driven Cavity Flow", Conference on Computational Mechanics and Simulation, ICCMS, IIT Guwahati, India, (2006).

[10] H.C. Kuhlmann, M. Wanschura, and H.J. Rath, "Flow in two-sided lid-driven cavities: no uniqueness, instability, and cellular structures", Journal of Computational Physics, vol. 336, PP. 267-299, (1997).

[11] S. Albensoeder, H.C. Kuhlmann, and H.C. Rath, "Multiplicity of Steady Two Dimensional Flows in Two-sided Lid-Driven Cavities", Theoretical Computational Fluid Dynamics, Vol. 14: PP. 223-241, (2001).

[12] C.H .Blohm, and H.C. Kuhlmann, "The two-sided lid-driven cavity: experiments on stationary and time-dependent flows", Journal of Fluid Mechanics, Vol. 450, PP. 67-95, (2002).

[13] A. A.R. Darzi, M. Farhadi, K. Sedighi, E. Fattahi and H. Nemati, "Mixed convection simulation on inclined lid driven cavity using Lattice Boltzmann method", Transactions of Mechanical Engineering, , Vol. 35, PP. 73-83, (2011).

[14] R. Begum and A. M. Basit, "Lattice Boltzmann Method and its Applications to Fluid Flow Problems", European Journal of Scientific Research, ISSN 1450-216X, Vol. 22(2), PP. 216-23, (2008).

[15] L. Currie, "Fundamental Mechanics of Fluids", university of Jodhpur (India), third Edition, (1977).

[16] J. L. Bansal, "Viscous Fluid Dynamics", university of toronto (Canada), (1977).

[17] Batchelor, George K, "An Introduction to Fluid Dynamics", Cambridge University Press, (1967)

[18] H. N.A. Ismail, "Selected Topics of Numerical Analysis and Scientific Computation", El mostapha Publishing house, Cairo, (2015)